Journal of the European Ceramic Society 23 (2003) 293–300

www.elsevier.com/locate/jeurceramsoc

Corrosion of high alumina and near stoichiometric spinels in iron-containing silicate slags

H. Sarpoolaky, S. Zhang, W.E. Lee*

University of Sheffield, Department of Engineering Materials, Mappin Street, Sheffield S1 3JD, UK

Received 12 January 2002; accepted 1 June 2002

Abstract

Dissolution of alumina-rich spinel aggregates in iron-containing silicate slag was studied using grain corrosion tests. High alumina spinels (AR90, 90% Al_2O_3) dissolve indirectly while dissolution of near stoichiometric (AR78, 78% Al_2O_3) spinel is entirely direct. This behaviour arises because higher alumina spinels can accommodate more cations from the slag due to the greater number of Mg^{2+} vacancies in their crystal structures. Removal of these cations increases the viscosity of the remaining silica-rich local slag so that alumina-rich spinels exhibit better penetration resistance. However, thermodynamic calculations predict that near stoichiometric spinel (AR78) is more corrosion resistant since more slag is needed to dissolve it completely.

Keywords: Corrosion resistance; $MgAl_2O_4$; Refractories; Slags

1. Introduction

Magnesium aluminate spinels (MA) have been extensively used in refractories because of their superior corrosion resistance and thermal shock resistance. Spinels are mixed oxide structures with general formulation of RO-R'_2O_3 (where R and R′ are a wide range of divalent and trivalent metal elements). The unit cell of MA can be expressed as $Mg_8Al_{16}O_{32}$ in which the 32 oxygen ions make a close packed cubic structure. Such close packing provides 64 divalent tetrahedrally- and 32 trivalent octahedrally-coordinated cation sites of which only 24 are filled so the spinel unit cell can be considered as a host cell capable of holding a large number of divalent and trivalent cations in solid solution.[1] According to the binary MgO–Al_2O_3 phase diagram, stoichiometric MA contains 28.2 wt.% MgO and 71.8 wt.% Al_2O_3. However, with increasing temperature, a wide range of non-stoichiometry may form in the system[1,2] and the solid solubility of alumina in spinel is higher than that of magnesia at the same temperature. For example, the solid solubilities of MgO and Al_2O_3 at 1600 °C are 2 and 6 wt.% respectively but increase to 3 and 10 wt.% at 1700 °C.[3]

Spinel may be produced commercially by heating a compacted mixture of magnesia and reactive alumina at elevated temperatures. Spinel formation is a heterogeneous reaction, which proceeds on both MgO–MA and Al_2O_3–MA interfaces by counter-diffusion of Al^{3+} and Mg^{2+} ions through the oxygen lattice.[4–7] Two forms of alumina-rich spinel grain (aggregates) are produced commercially with 22–23 wt.% or 9–10 wt.% MgO. The latter is more often used as an aggregate in refractory castables due to its good high temperature and corrosion-resisting properties and lower thermal spalling.

In alumina-rich spinel grain raw materials alumina is not necessarily present as a free second phase but in solid solution decreasing the spinel lattice parameter, which can be used to estimate the extent of non-stoichiometry in an alumina–spinel compound.[5,8] However, thermal shock behaviour, slag penetration resistance and wear of the alumina-rich spinel are improved by the presence of free alumina.[9,10]

Slag attack of refractories involves both penetration (physical permeation via open porosity and grain boundaries) and corrosion (penetration and chemical reaction often dissolution). Bates[11] studied dissolution of spinel in a calcium aluminosilicate (CAS) slag from =1300 to 1600 °C. He showed that gehlenite and anorthite formed as boundary layer phases depending on the slag composition. Bahram and Barrett[12] had earlier

* Corresponding author.
E-mail address: w.e.lee@sheffield.ac.uk (W.E. Lee).

0955-2219/02/$ - see front matter
PII: S0955-2219(02)00170-X

suggested spinel dissolution was indirect. Oh et al.[13] compared dissolution and slag penetration of polycrystalline alumina and spinel grains by immersing them in a CAS slag and showed that the slag entered the spinel grain and grain boundaries while the iron diffused into the spinel leading to a change in slag composition and consequently to an increase in the slag viscosity. The compositions of the penetrated (local) slag in the spinel and alumina were different although the bulk slag composition was similar, emphasising the importance of the concept of local liquid composition in such corrosion studies.[14] The present authors studied dissolution of alumina-rich spinels in a model calcia magnesia aluminosilicate (CMAS) melt.[15] The higher alumina spinel showed better penetration resistance whereas thermodynamic calculations suggested that the lower alumina spinel might have better corrosion resistance. Very recently, Cho et al.[21] examined corrosion of alumina-rich, MgO-rich and stoichiometric spinel grains (clinkers) by a CAS ladle slag after 5 min hold times and determined the mechanisms to be predominantly indirect via formation of complex spinel interlayers.

However, detailed studies of the penetration and corrosion resistance of alumina-rich spinels in contact with complex and commercially relevant iron-containing silicate slags for extended times have not been previously performed.

2. Experimental procedure

Two commercial sintered alumina-rich magnesium spinels, AR90 (90 wt.% Al_2O_3), AR78 (78 wt.% Al_2O_3) were supplied by Alcoa Industrial Chemicals, Frankfurt, Germany. The supplier's analysis (Table 1), reveals the main impurities in both grains were CaO, SiO_2 and Na_2O. CaO and SiO_2 were higher in AR78 than in AR90, but Na_2O was lower. The apparent porosities in both grains were similar. A complex model EAF slag with a composition shown in Table 2 was prepared using calcium carbonate ($CaCO_3$) and magnesium carbonate ($MgCO_3$) from BDH Laboratory supplies (Poole, UK), iron oxide (Fe_2O_3), manganese oxide (MnO) and alumina from Aldrich Chemical Co., (Gillingham, UK) and Loch Aline silica sand (SiO_2) supplied by Tilcon (Stoke, UK).

Table 1
Chemical composition (wt.%) and physical properties of spinels (suppliers' data)

	AR90	AR78
Al_2O_3	90	76
SiO_2	0.03–0.1	0.08–0.12
MgO	9–10	22–23
MnO	–	–
Fe_2O_3	0.05–0.08	0.06–0.09
CaO	0.12–0.16	0.22–0.26
Na_2O	0.13–0.17	0.06–0.12
Porosity (Vol.%)	1.5–2.5	1.5–2
Bulk density (g cm^{-3})	3.38–3.42	3.25–3.29

Corrosion tests were carried out using two alumina crucibles containing the aggregates (~10 mm dia.), one in each, which were filled with powdered slag and heated in air to 1600 °C in an electric furnace at 5 °C / min and held for 15 min. The furnace was then switched off and naturally cooled to room temperature. The corroded samples were sectioned perpendicular to the spinel/slag interface, and impregnated with resin, ground and polished, and carbon-coated using standard ceramographic techniques. Secondary electron (SEI) and back-scattered electron imaging (BSI) were done on an SEM (Camscan Electron Optics, Waterbeach, Cambridge, UK) equipped with an EDS analyser (Model No. AN10000, Link Systems, High Wycombe, Buckinghamshire, UK). Dot mapping was carried out to study the phase distribution formed in corroded AR90 grain using a LEO 438 VP SEM equipped with a Rontec multimax plus flash detector.

The thermodynamic calculations were conducted with the DOS version 2.0 of the FACT package.[16] The effect of slag attack was modelled by successive additions of slag to the refractories, monitored by the parameter alpha. For alpha = 2, the calculations were carried out with 100 g of the refractory spinel and 200 g of slag. Slag model A (SLAGA) allowed solution of MgO, FeO, MnO, Na_2O, SiO_2, CaO, TiO_2, Ti_2O_3 and Al_2O_3 in the oxide melt. The model SOLN-AL_2O_3 was used for alumina, which allows solution of FeO and MnO and the model SOLN-SPINEL was used for the spinel solutions ($MgAl_2O_4$, $MnAl_2O_4$ and $FeAl_2O_4$). Sarpoolaky et al.[17] describe details of using FACT to predict the species formed in corrosion of refractories.

3. Results

3.1. Thermodynamic calculations

Fig. 1 shows predicted species in the spinel–slag systems at 1600 °C. In AR90, alumina and spinel are present as two solid phases before the dissolution starts (Fig. 1a). The levels of alumina and spinel decrease with increasing alpha and abruptly drop to zero at alpha 0.4 and 0.8 respectively revealing their complete dissolution in the slag. Since alumina dissolves in less slag it can be said to dissolve more easily. In AR78 (Fig. 1b) no free alumina phase is predicted, only solid solution spinel. With increasing alpha, its level decreases until alpha ~1, when it decreases to zero, indicating that it completely dissolves in the slag. The predicted compositions of the spinel solutions in AR90 and AR78 during dissolution are shown in Fig. 2. AR78 initially contains more

Table 2
Chemical composition of as-mixed model slag (wt.%)

	CaO	Al_2O_3	SiO_2	Fe_2O_3	MgO	MnO	CaO/SiO_2 (mole)
Model slag	32.37	12.47	23.49	17.49	5.9	8.88	1.48

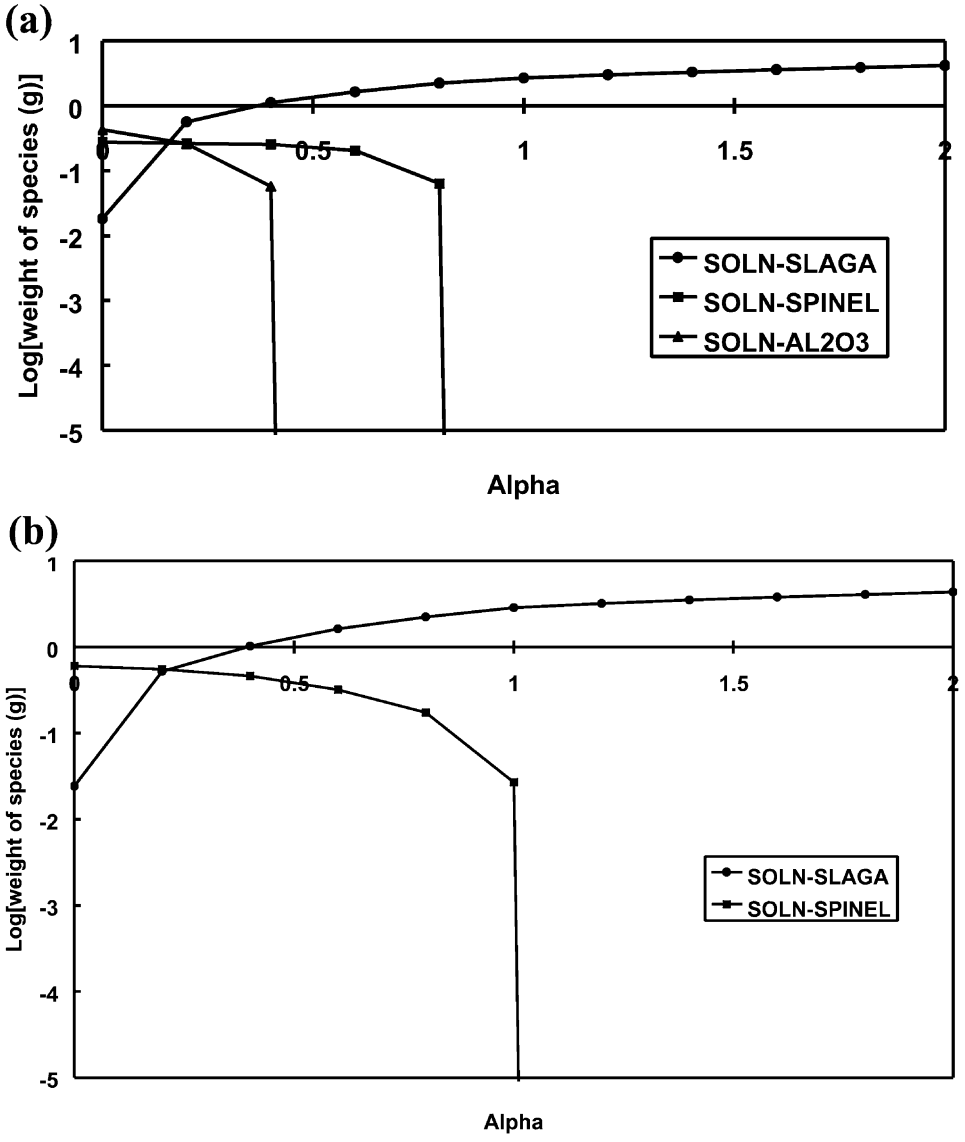

Fig. 1. Predicted species from slag attack at 1600 °C for (a) AR90 and (b) AR78 showing slag solid solutions (SOLN-SLAGA), alumina (SOLN-AL_2O_3) and spinel (SOLN-SPINEL) coexisting and Al_2O_3 dissolving in less slag than spinel (a).

MA and does so throughout the dissolution process. Fe and Mn spinels [($FeAl_2O_4$) and ($MnAl_2O_4$)] form in both AR78 and AR90 but the equilibrium level of Mn spinel formed is higher than Fe spinel (indicated by its higher slope in Fig. 2). The level of Mn spinel in AR90 is predicted to be slightly lower than in AR78 during the early stages of dissolution but becomes much larger when alpha is between 0.4 and 0.8. Similarly, a larger amount of Fe spinel is formed in AR90 with alpha between 0.45 and 0.65. When alpha = 0.65 in AR90 the Mg, Mn and Fe spinel contents abruptly drop to zero while this does not happen in AR78 until alpha = 1 indicating that the spinel formed in AR90 dissolve in the slag more easily than that of AR78.

3.2. X-ray diffraction (XRD)

XRD of the spinel aggregates revealed α-alumina and magnesium aluminate spinel as the main phases in AR90, while in AR78 only magnesium aluminium

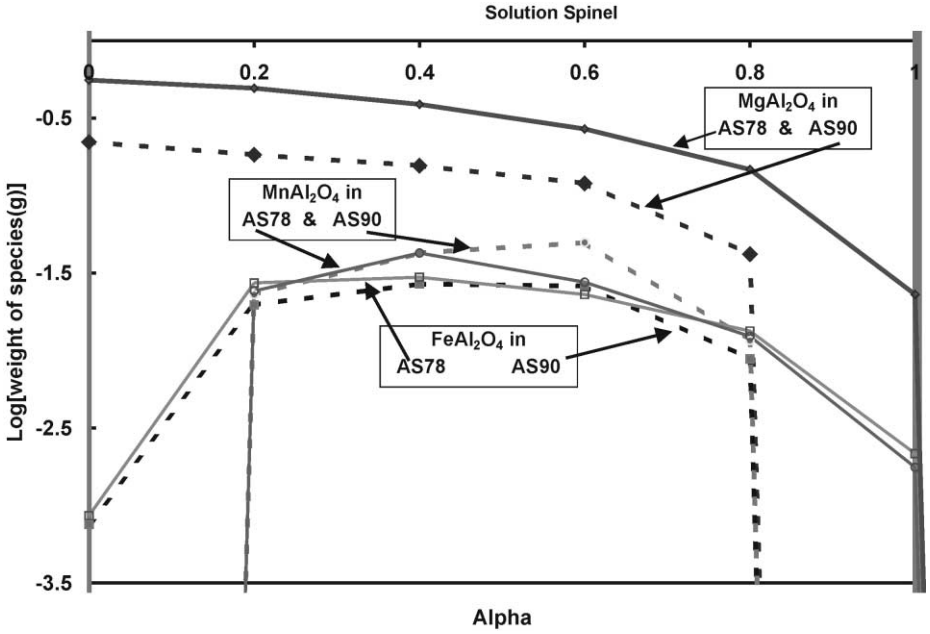

Fig. 2. Composition of spinel solution (SOLN-SPINEL) in AR90 (dotted line) and AR78 (solid line) showing that levels of $MnAl_2O_4$ and $FeAl_2O_4$ in spinel solid solution (SOLN-SPINEL) in AR78 are higher than in AR90 during the early stages of attack although their levels in AR90 exceed those in AR78 later. Note spinels labelled AS rather than AR in this figure.

spinel was found. The as-cooled model slag contained spinel, which EDS analysis revealed as complex spinel containing manganese and iron oxides [(Mg, Fe, Mn)(Al, Fe)$_2$O$_4$], and melilite which is a solid solution of gehlenite (C_2AS) and akermanite (C_2MS_2).

3.3. Microstructures

3.3.1. Uncorroded microstructures

Sintered AR90 grain (Fig. 3) contains intergranular pores up to 5 μm dia. and larger intragranular pores up to 10 μm dia. AR90 contained lath-shaped corundum (30 μm long and 10 μm wide) along with angular spinel (~40 μm). Sintered AR78 (Fig. 4) contains spinel grains together with calcium aluminate, which EDS suggested was calcium hexaluminate (CA_6). CA_6 formation can be attributed to reaction of alumina in the spinel with CaO impurity from the raw material (Table 1). Careful SEM/EDS analysis revealed the presence of low melting CMAS phases at the grain boundaries of AR78.

BSI of the as-melted slag after 1 h at 1600 °C (Fig. 5) revealed bright dendrites of hercynitic spinel [(Mg, Mn, Fe)(Al, Cr, Fe)$_2$O$_4$] with grey melilite in a CAS matrix which is presumably glass. The weighted average atomic numbers of the gehlenite and akermanite are similar (~13.1) so differences in contrast of melilite can be related to the level of MnO and Fe_xO as the lighter regions contain higher levels of these oxides.[18]

3.3.2. Corroded microstructures

The microstructure of the AR90/slag interface after 15 min corrosion at 1600 °C (Fig. 6) reveals a discontinuous and thin CA_6 (10 μm) layer adjacent to the grain together with a thick (150–200 μm) spinel layer containing CAS. EDS revealed that the lighter contrast of the spinel layer adjacent to the bulk slag was due to higher iron and manganese oxide contents.

The distribution of Fe, Mn, Mg, Ca, Al and O in the microstructure of AR90 corroded by slag is shown in the X-ray dot maps of Fig. 7. Large amounts of Fe and Mn are absorbed in the grain-slag interface fading through the grain. The bright edge of the boundary layer in contact with the slag is rich in Fe and Mn. EDS analysis showed that the CAS islands in the boundary layer are silica-rich and lower in Fe and Mn compared to the bulk slag indicating that the trapped slag in the

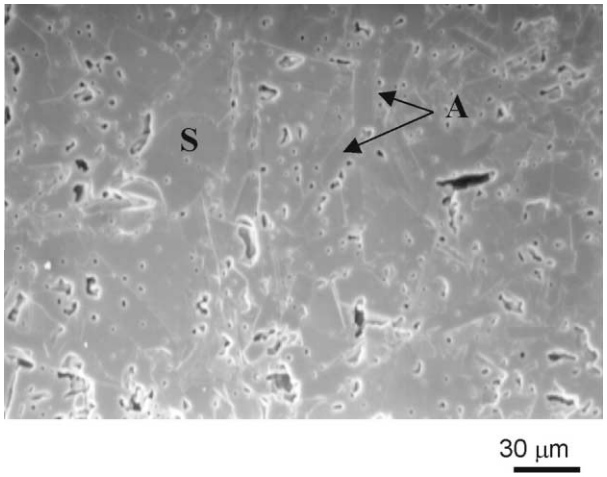

Fig. 3. BSI of AR90 showing angular spinel (S) and alumina laths (A) with inter- and intra-granular pores.

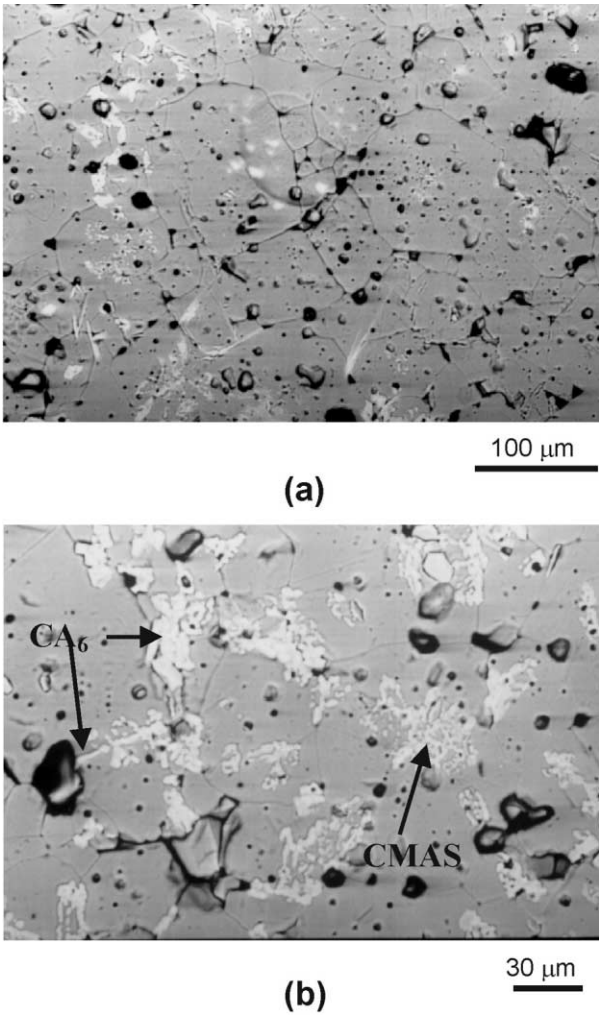

Fig. 4. BSI of AR78 showing (a) angular spinel grains and CA_6 and (b) CA_6 and CMAS phases at grain boundaries.

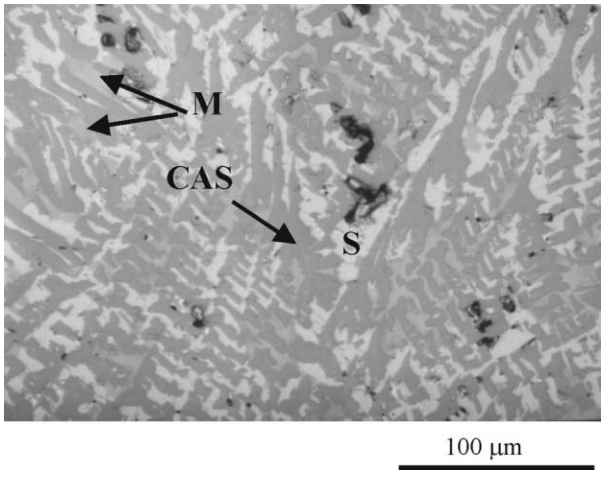

Fig. 5. BSI of slag after 1 h at 1600 °C, showing hercynitic spinel (bright dendrites, S), grey melilite (M) and calcium aluminosilicate (CAS) matrix.

interface has lost some of Fe, Mn and Ca so becoming silica-rich and viscous. This indicates that some of the Al, Fe, Mn and Mg ions of the CAS islands were taken by spinel phases in the grain boundary matrix leaving the melt in CAS islands more viscous.

Slag penetrated deeply (1.5 mm) in AR78 via pores and grain boundaries after 15 min at 1600 °C (Fig. 8). A single hercynitic spinel layer was detected as a boundary layer adjacent to the grain. The lighter contrast edges are the same phase but richer in iron and manganese ions. The bulk slag contains spinel and melilite crystals. The spinel boundary layer in AR78 was non-uniformly thin and discontinuous.

4. Discussion

Although the alumina content of AR78 is greater than that of stoichiometric spinel MA (71.8 wt.%),

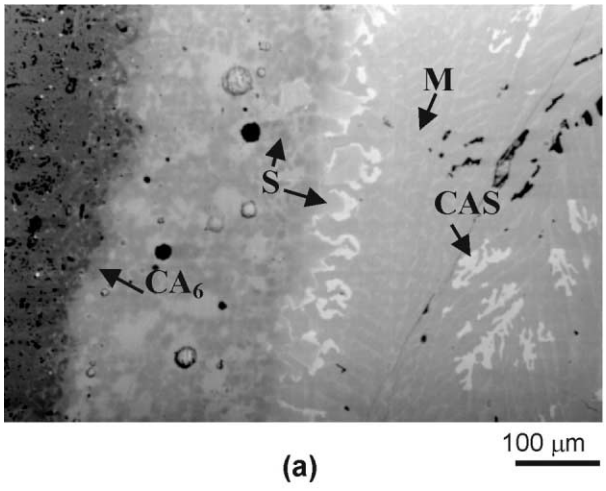

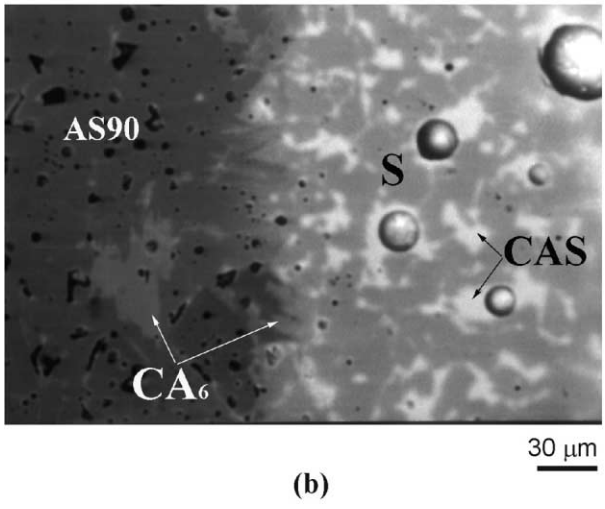

Fig. 6. (a) BSI of corroded AR90 grain (labelled AS90) after 15 min at 1600 °C showing thin CA_6 layer adjacent to the spinel grain and a spinel layer containing CAS and slag phases, melilite (M) and CAS, (b) higher magnification of the interface.

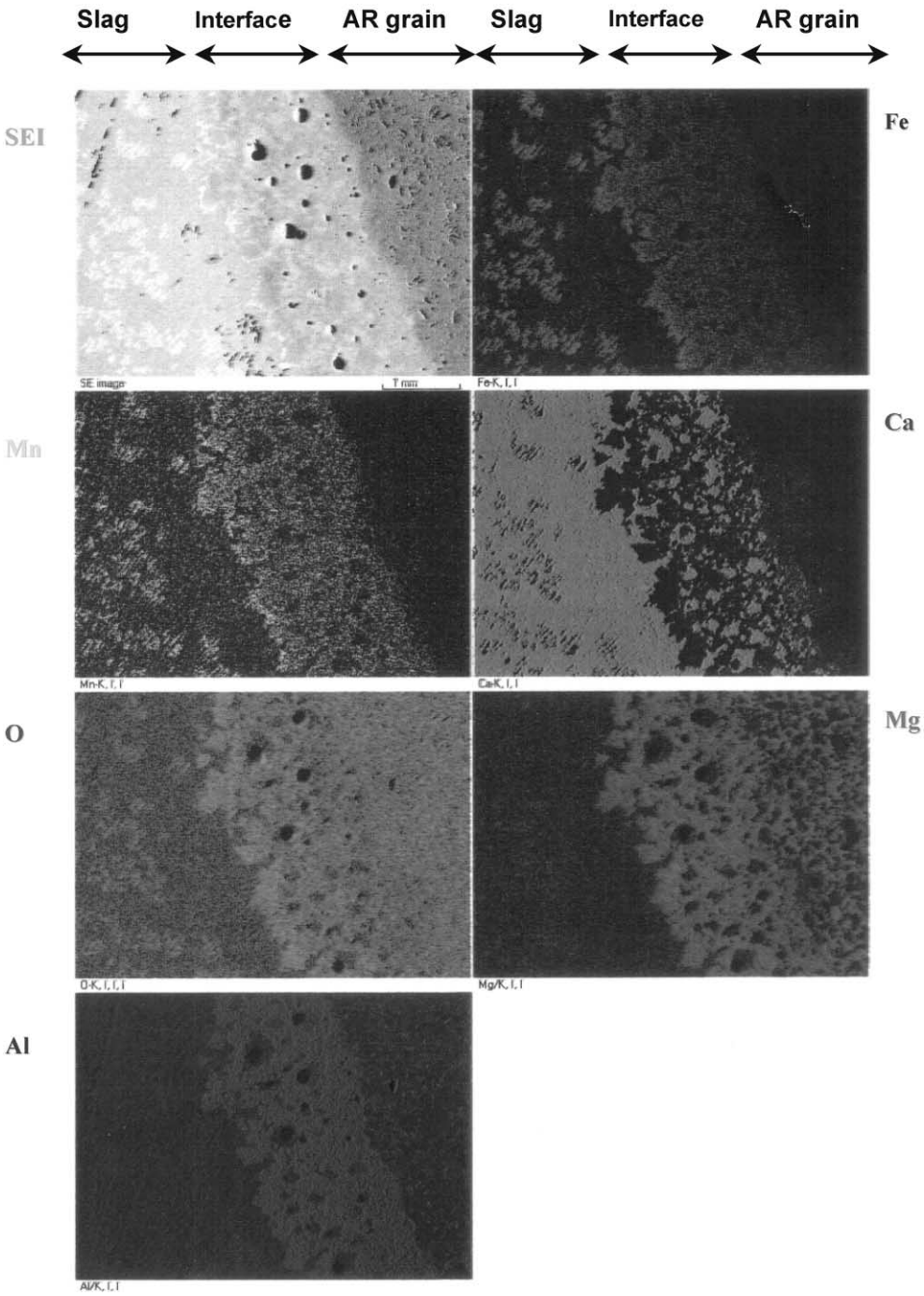

Fig. 7. X-ray dot maps of AR90 grain corroded by slag at 1600 °C showing distribution of various ions in the grain, interface and slag.

thermodynamic calculations (Fig. 1b) predict that no free alumina is present in it at 1600 °C, indicating that at this temperature excess Al_2O_3 reacts with MA to form an Al_2O_3-rich spinel. On the other hand, the higher level of Al_2O_3 in AR90 cannot be accommodated in solid solution so free alumina is predicted (Fig. 1a, b). Thermodynamic predictions also show (Fig. 1) that solid alumina and/or spinel contents decrease with increasing level of slag (alpha) in both, suggesting that AR90 and AR78 were not saturated with the main elements of the slag. This is confirmed by comparing the corroded microstructures (Figs. 6 and 8) with that of the slag alone (Fig. 5) which show that after corrosion at 1600 °C new product phases, such as CA_6 and spinel, formed at the grain/slag interfaces.

Generally, when a refractory grain and a slag come into contact dissolution and interdiffusion processes are initiated in both, which in indirect dissolution may lead to formation of a boundary layer adjacent to the refractory grain. The concentration distribution in this

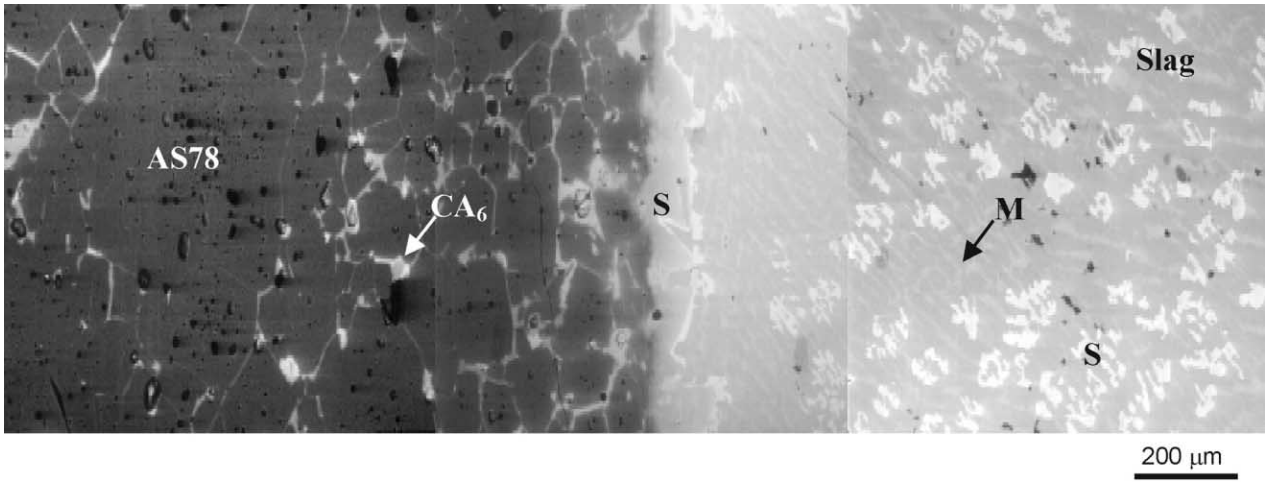

Fig. 8. BSI of corroded AR78 grain (labelled AS78) after 15 min at 1600 °C showing deep slag penetration into the grain and a spinel layer (S) whose edge is iron-rich. The slag contains CA_6, hercynitic spinel (S) and melilite (M) in what is believed to be a glassy matrix.

boundary layer depends on the mobility of the diffusing species in the molten slag and the refractory. Corrosion of alumina grain in CAS slag[15] involves early reaction of CaO from the slag with alumina in the grain to form CA_6 since Ca is transported more quickly to the grain/slag interface than other cations. Similarly, a thin CA_6 layer was formed adjacent to the AR90 during the dissolution process (Fig. 6). In AR78 no CA_6 was found at the grain/slag interface although it was detected in the slag-penetrated region indicating that Ca^{2+} from the slag reacted with alumina in the AR78, which is not free alumina, and formed CA_6 that will later dissolve into the slag. This observation is supported by thermodynamic calculations, which do not predict CA_6, so it is likely to react with adjacent SiO_2 and alumina to form low melting CAS phases (Fig. 1).

The thermodynamic predictions (Fig. 2) revealed a gradual increase in levels of Fe and Mn in the spinel solid solutions (SOLN-SPINEL) with increasing slag content (alpha) More Mn than Fe was incorporated into the spinel. Higher levels of Fe and Mn were predicted in the spinel solid solution of AR78 than that of AR90 early in the dissolution process when alpha 0.4. On increasing the level of slag, larger amounts of Mn and Fe were predicted to occur in the spinel solid solution of AR90 until their levels exceed those of spinel in AR78 (Fig. 2). This can be explained by the higher equilibrium level of spinel formation in AR90 due to a greater number of Mg^{2+} vacant positions present in the alumina-rich spinel crystal structure, which is believed to absorb more ions from the slag acting as a sink for unwanted slag ions.[19] When most of the iron and manganese ions diffuse into the spinel the slag adjacent to the spinel surface becomes (locally) silica-rich and viscous, limiting the slag penetration.[19] More alumina-rich spinels can accommodate greater levels of divalent ions from the slag forming thicker complex (hercynitic) spinel layers compared to stoichiometric spinel.[19] Meanwhile alumina from the spinel consumes CaO from the slag to form CA_6 making the local slag silica-rich thus increasing local slag viscosity and, consequently, suppressing slag penetration.[9,15]

Alumina-rich spinel AR90 formed a thick and nearly continuous hercynitic spinel layer at the interface with the slag and hence showed increased resistance to slag penetration than AR78 at 1600 °C. The grain dissolution in AR90 appears to be indirect as the Mg spinel absorbs iron and manganese to form Mn and Fe-containing spinel solid solution which may, however, eventually form low melting iron spinel (Fe_3O_4)[20] which more easily dissolves in the slag. The level of Fe and Mn ions taken up at the interface layer and its thickness are the critical factors in the long-term corrosion of the AR90.

Extensive slag penetration was detected in AR78 mainly through the grain boundaries. A thin and discontinuous hercynitic spinel was detected at the grain-slag interface with some CA_6 in the penetrated grain boundaries, which could be a result of reaction of Ca from the slag with the dissolved alumina in the spinel grain AR78 (Fig. 8). As shown in Table 1 the uncorroded AR78 contained relatively high levels of Ca, Si as impurities which formed CA_6 and low melting CMAS in the grain boundaries. It is difficult to distinguish between these two forms of CA_6 in the SEM microstructure. Possibly some of the existing CA_6 in the grain boundaries dissolved in the slag while some was newly formed by reaction of the slag and alumina in the grain.

AR78 was penetrated more deeply by the slag than AR90 attributable to two main reasons. Firstly, in AR78, the CMAS phases at the grain boundaries were most likely liquid at the test temperature, facilitating the slag penetration. Secondly, slag viscosity in AR78 was lower than that of AR90. CaO from the slag was consumed by alumina in AR90 to form the CA_6 layer at the grain/slag interface. Also as the experimental and

thermodynamic results show AR90 absorbed higher levels of Fe and Mn oxides from the slag than AR78 so the slag local to AR90 contains less Ca, Fe and Mn oxides and is more silica-rich and viscous during the corrosion test. As the boundary layer in AR78 was thin and discontinuous dissolution of this grain was clearly direct along with high slag penetration into it.

The corrosion resistance of the spinel grains was not quantitatively compared in this test. Nevertheless, the thermodynamic calculations (Fig. 1) give some clues. As shown in Fig. 1, AR90 dissolves completely in the slag when alpha reaches about 0.8, while AR78 does not dissolve completely until alpha reaches 1, suggesting that AR78 should have better corrosion resistance (in terms of dissolvability) than AR90 since more slag is needed to dissolve it.

5. Conclusions

1. Alumina, either free or as solid solution in spinel, reacts with calcia from iron-containing silicate slag and forms CA_6 which further reacts with SiO_2 from the slag to form low melting CAS.
2. The magnesium–aluminate spinel crystal structure takes up Fe^{2+} and Mn^{2+} from the slag leading to formation of a layer of complex (hercynitic) spinel depressing slag corrosion by dissolving indirectly into the slag. Further dissolution of iron oxides may lead to formation of low melting spinel phases.
3. Due to 1 and 2 the dissolution of AR90 in the iron-containing silicate slag is suggested to be indirect at 1600 °C.
4. Dissolution of AR78 was direct as the spinel layer formed adjacent to the grain was discontinuous and thin.
5. AR90 shows better slag penetration resistance than AR78 while thermodynamic calculations suggested better corrosion resistance in AR78.

Acknowledgements

The authors thank EPSRC, UK (grant GR/L57852), and H.S. thanks the Iran University of Science and Technology (IUST), for their support.

References

1. Ulmer, G. C., Chromium spinel. In: *High Temperature Oxides, Part I, Magnesia, Lime and Chromium Refractories*, ed. A. M. Alper. New York, USA, 1970, pp. 252–315.
2. Vishnevskii, I. and Skirpak, V. N., Scattering of phonons by cation vacancies in spinel. *Soviet Physics-Solid State*, 1966, **7**(10), 2374–2378.
3. Serry, M. A., Hammad, S. M. and Zawrah, M. F. M., Phase composition and microstructure of refractory $MgAl_2O_4$ spinel grains. *Br. Trans. Soc.*, 1998, **79**(6), 175–183.
4. Fuhrer, M., Hey, A. and Lee, W. E., Microstructural evolution in self-forming spinel/calcium aluminate-based castable refractories. *J. Eur. Ceram. Soc.*, 1998, **18**, 813–820.
5. Bailey, J. H. and Russell, R., Preparation and properties of dense spinel ceramics in the $MgAl_2O_4$-Al_2O_3 system. *Trans. Br. Ceram. Soc.*, 1969, **68**, 159–164.
6. Rigaud, M., Palco, S. and Wang, N., Spinel formation in the MgO-Al_2O_3 system relevant to basic castables. In: *Proceedings of the Unified Int. Tech. Conf. on 'Refractories' (UNITECR '95)*. Kyoto, Japan, 1995, pp. 387–392.
7. Cunha, F. N. and Bradt, R. C., Reaction constituents for in-situ bonds of $MgAl_2O_4$, Mg_2SiO_4 & $3Al_2O_3.2SiO_2$ in refractories. In *Proceedings of the 57th Electric Furnace Conference*. Pittsburg, PA, 1999, pp. 143–152.
8. Shirasuka, K. and Yamaguchi, G., Precise measurment of the crystal data and the solid solution range of the defective spinel MgO-nAl_2O_3. *Yogyo-Kiokai-Shi*, 1974, **82**(12).
9. Sumimura, S., Yamamura, T., Kubata, Y. and Kaneshige, T., Study on slag penetration of alumina-spinel castable. In: *Proceedings of the Unified Int. Tech. Conf. on 'Refractories' (UNITECR '91)*. Aachen, Germany, 1991, pp. 97–101.
10. Korgul, P., Wilson, D. R. and Lee, W. E., Microstructural analysis of corroded alumina-spinel-castable refractories. *J. Eur. Ceram. Soc.*, 1997, **17**, 77–84.
11. Bates, J. L., Heterogeneous dissolution of refractory oxide in molten calcium aluminum silicates. *J. Am. Ceram. Soc.*, 1987, **70**(3), C55–C57.
12. Bahram, D. and Barrett, L. R., The dissolution of magnesium aluminate spinel in sodium silicate melts. *Trans. Br. Ceram. Soc.*, 1968, **67**, 49–56.
13. Oh, T.-I., Shen, L. M., Ure, R. W. and Cutler, I. B., Slag penetration into oxide refractories. *Am. Ceram. Soc. Bull.*, 1977, **56**(7), 649–650.
14. Lee, W. E. and Zhang, S., Melt corrosion of oxide and oxide-carbon refractories. *Int. Mater. Rev.*, 1999, **44**(3), 77–104.
15. Zhang, S., Sarpoolaky, H. and Lee, W. E., Dissolution of $MgAl_2O_4$ (MA) spinel grain in CaO-MgO-Al_2O_3-SiO_2 melt. In: *Proceedings of the 44th International Colloquium on Refractories*. Aachen, Germany, 2001, pp. 64–67.
16. Bale, C. W. and Pelton, A. D., *FACT-Win-User Manual*. CRCT, Ecole Polytechnique de Montreal, Qebec, Canada (http://www.crct.polymtl.ca, 1999).
17. Sarpoolaky, H., Zhang, S., Argent, B. B. and Lee, W. E., Influence of grain phase on slag corrosion of low cement castable refractories. *J. Am. Ceram. Soc.*, 2001, **84**(2), 426–434.
18. Zhang, S., Rezaie, H. R., Sarpoolaky, H. and Lee, W. E., Alumina dissolution into silicate slag. *J. Am. Ceram. Soc.*, 1999, **83**(4), 897–903.
19. Matsumoto, O., Isobe, T., Nishitani, T. and Genba, T., *Alumina-spinel Monolithic Refractories. US Patent, 4990475*. Harima Ceramic Co, Nippon Steel: USA, 1991.
20. Pandit, S. S. and Jacob, K. T., Spinel deoxidation equilibria in the Fe-Mn-Al-O system: experiment and computation. *Steel Res.*, 1987, **58**(3), 105–110.
21. Cho, M.-K., Hong, G.-G. and Lee, S.-K., Corrosion of spinel clinker by CaO-Al_2O_3-SiO_2 ladle slag. *J. Eur. Ceram. Soc.*, 2002, **22**, 1783–1790.